Supplement of Earth Surf. Dynam., 12, 163–180, 2024
https://doi.org/10.5194/esurf-12-163-2024-supplement

Supplement of

Past anthropogenic land use change caused a regime shift of the fluvial response to Holocene climate change in the Chinese Loess Plateau

Hao Chen et al.

Correspondence to: Xianyan Wang (xianyanwang@nju.edu.cn) and Ronald Van Balen (r.t.van.balen@vu.nl)

S1: The reconstructions of natural discharge and sediment load

The reconstructions of natural discharge and sediment load for each hydrological station in the study area are based on the calculated data from Chang et al. (2016). They determined the natural discharge and sediment load data for five hydrological stations (the lingjiacun, xianyang, huaxian, zhangjiashang and zhuangtou stations) in the Wei River catchment since 1990s, based on the double-mass curves method (DMCs). The DMCs calculated the natural discharge and sediment load by analyzing the correlations between cumulative precipitation and annual discharge or sediment load (Walling, 2006). Then, the ratios between these five stations and the others were calculated based on the observed mean annual discharge or sediment load data collected from the literature (Zhang et al., 2007; Ran et al., 2012; Wang, 2013; Chen, 2017; Han, 2019). Since the contributions of dams to each hydrological station were similar (Chang et al., 2016), we calculated the natural discharge and sediment load for all hydrological stations in the Wei River catchment by multiplying the reconstructed data in those five stations and the ratios between them and the others (Table S3).

S2: The validation for reconstructions of Holocene precipitation and air temperature

The trend of annual air temperature and monsoon precipitation over the last 5000 years in the Beilianchi lake were established by analyzing the branched glycerol dialkyl glycerol tetraethers (brGDGTs) (Zhang et al., 2021) and leafwax hydrogen isotope (C. Zhang et al., 2020), respectively. The dynamic downscaling modelling results on the millennial scale climate of China were also brought into contrast to make a more comprehensive consideration (Fig. S2). The simulated results were calculated by the CESM model, which used the monthly mean atmospheric circulation data of the fully-forced transient experiment results (TraCE-21ka) as lateral boundary nested into the regional climate model (RegCM4) (Kuang et al., 2021). The compared results showed that the predicted data calculated by assuming the Holocene climate patterns were same as the present-day were closer to the reconstructed data in the Beilianchi lake (Fig. S2). Therefore, it is better to apply these climate data in the Holocene simulations.

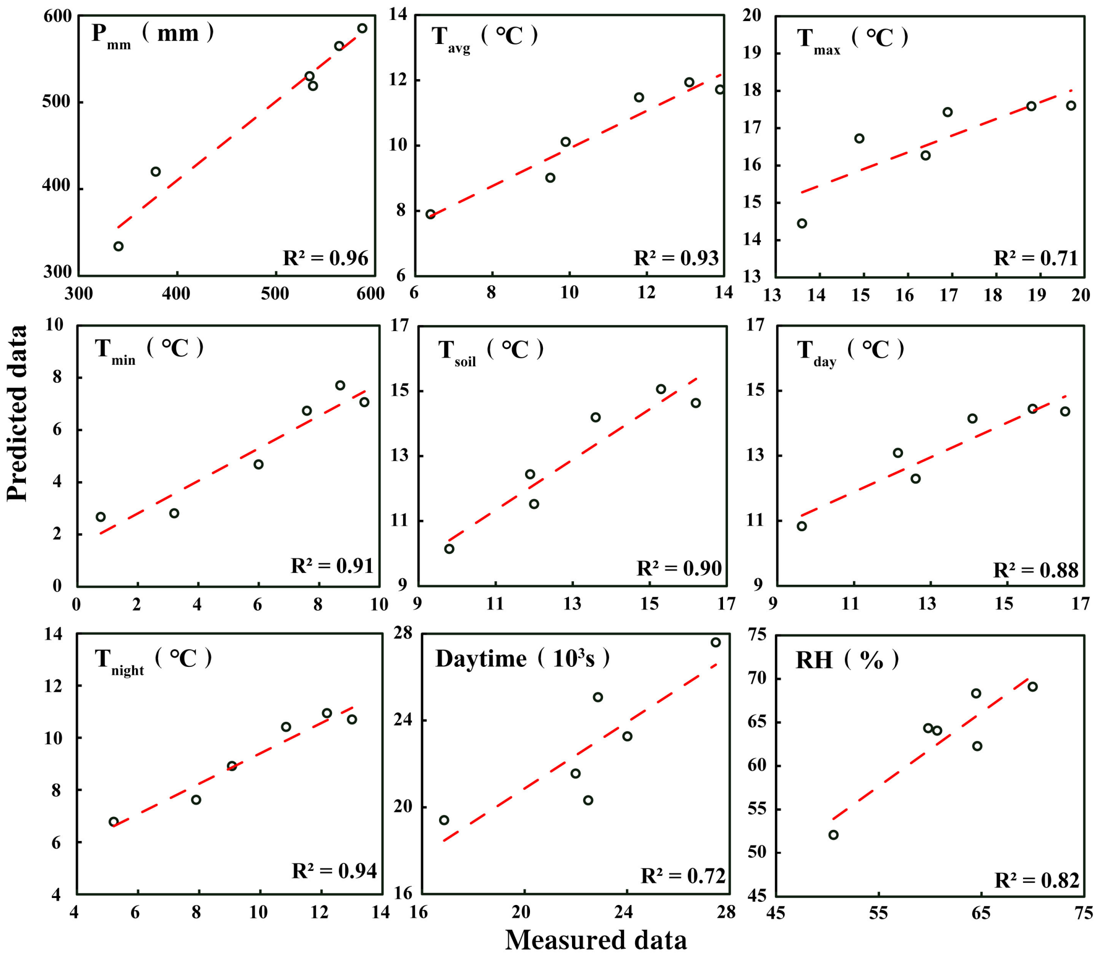

Fig S1 Scatter plot of predicted and observed meteorological data at the validation stations in Wei River catchment

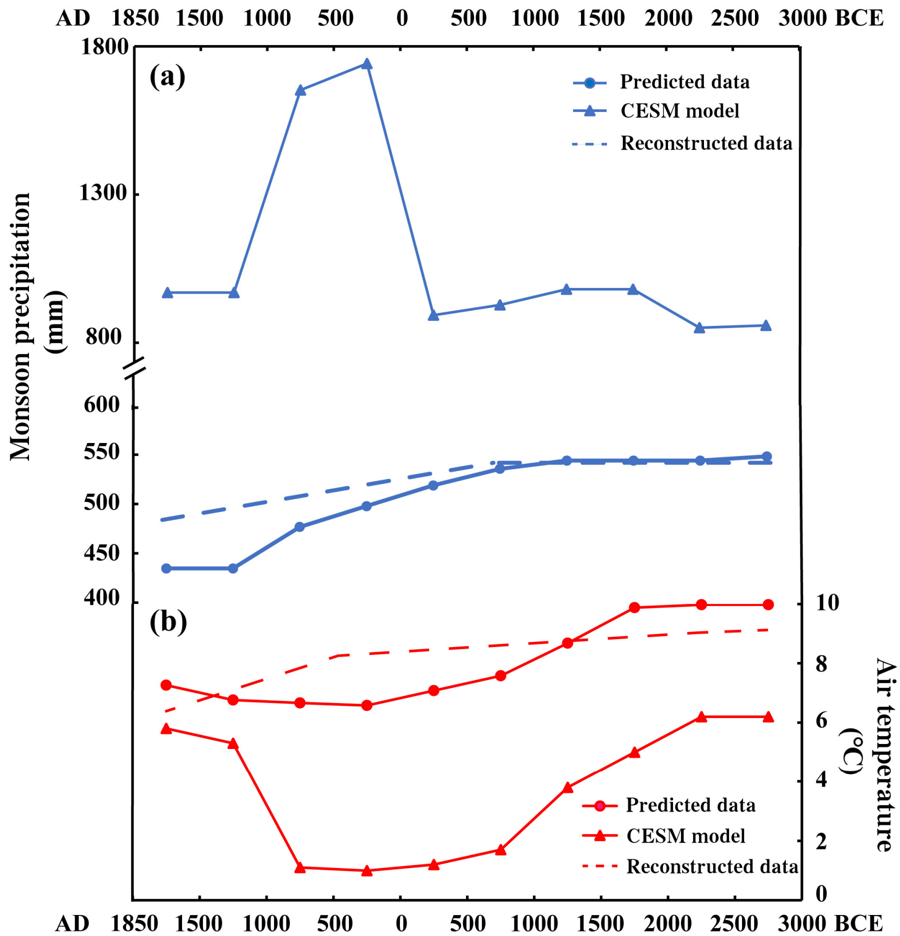

Fig S2 The predicted, CESM modelling and reconstructed monsoon precipitation (a) and mean annual air temperature (b) at Beilianchi lake within the Wei River catchment

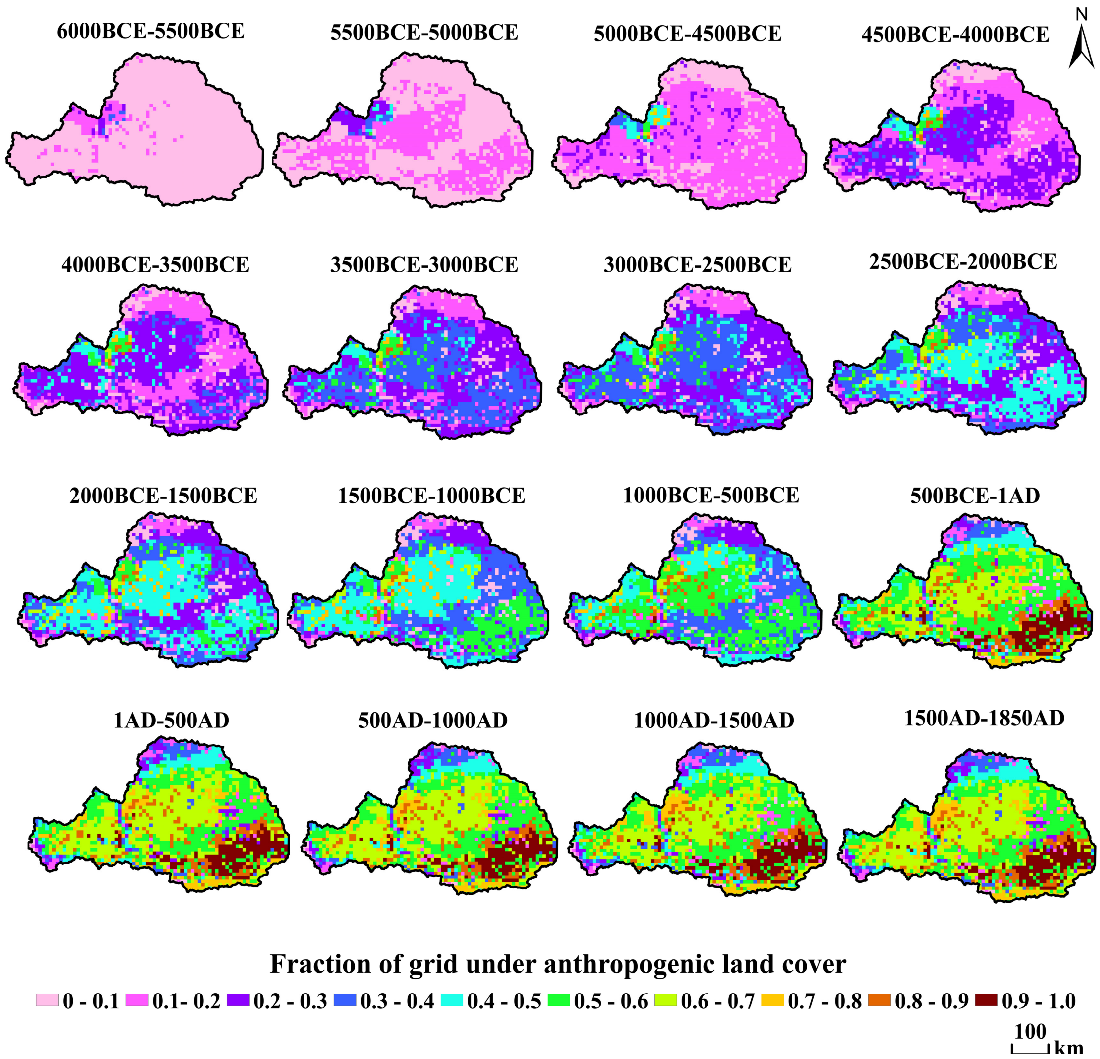

Fig S3 Anthropogenic land use cover map in Wei River catchment, from 6000BCE to 1850AD

(modified from Kaplan et al., 2011)

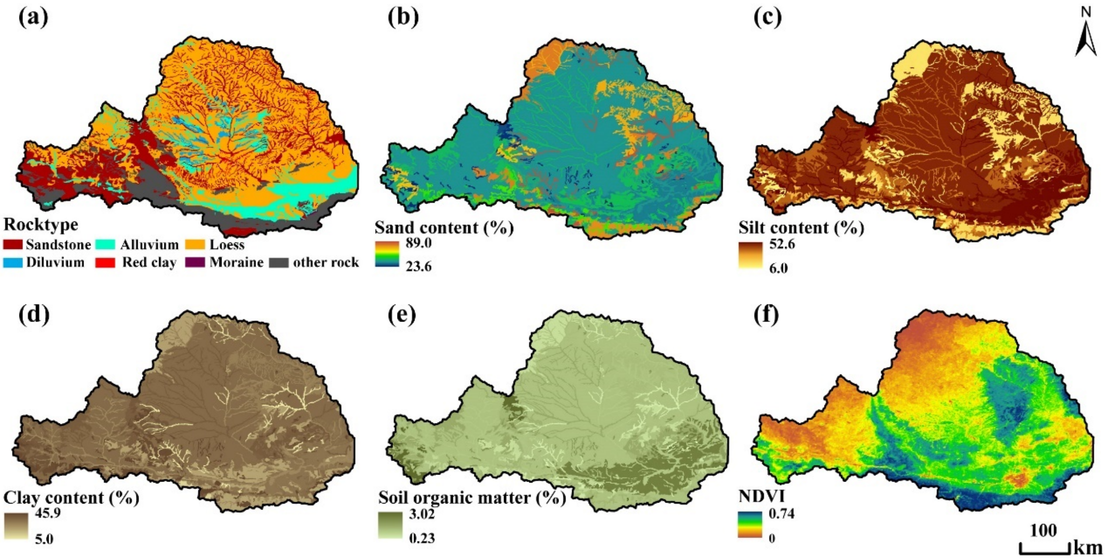

Fig S4 Distribution of rock types (a), sand (b), silt (c), clay (d), soil organic matter (e) content and NDVI data (f) in Wei River catchment.

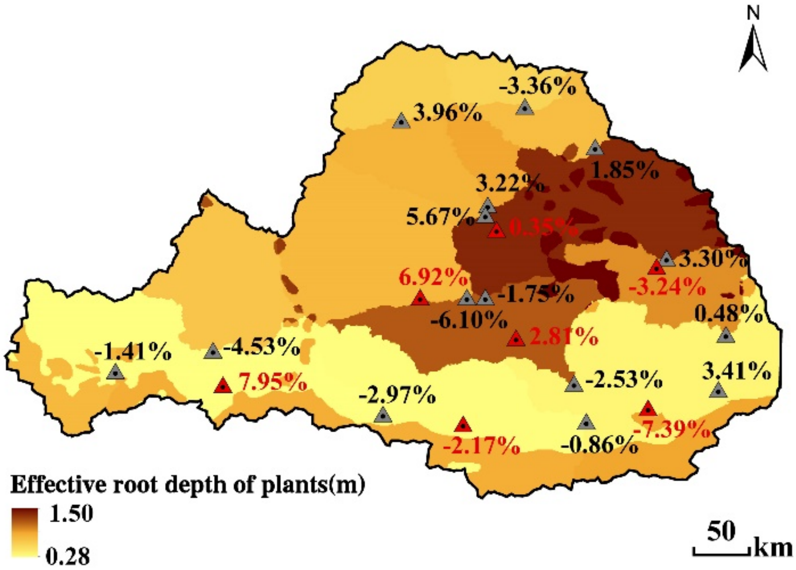

Fig S5 The distribution of effective root depth of plants after calibration

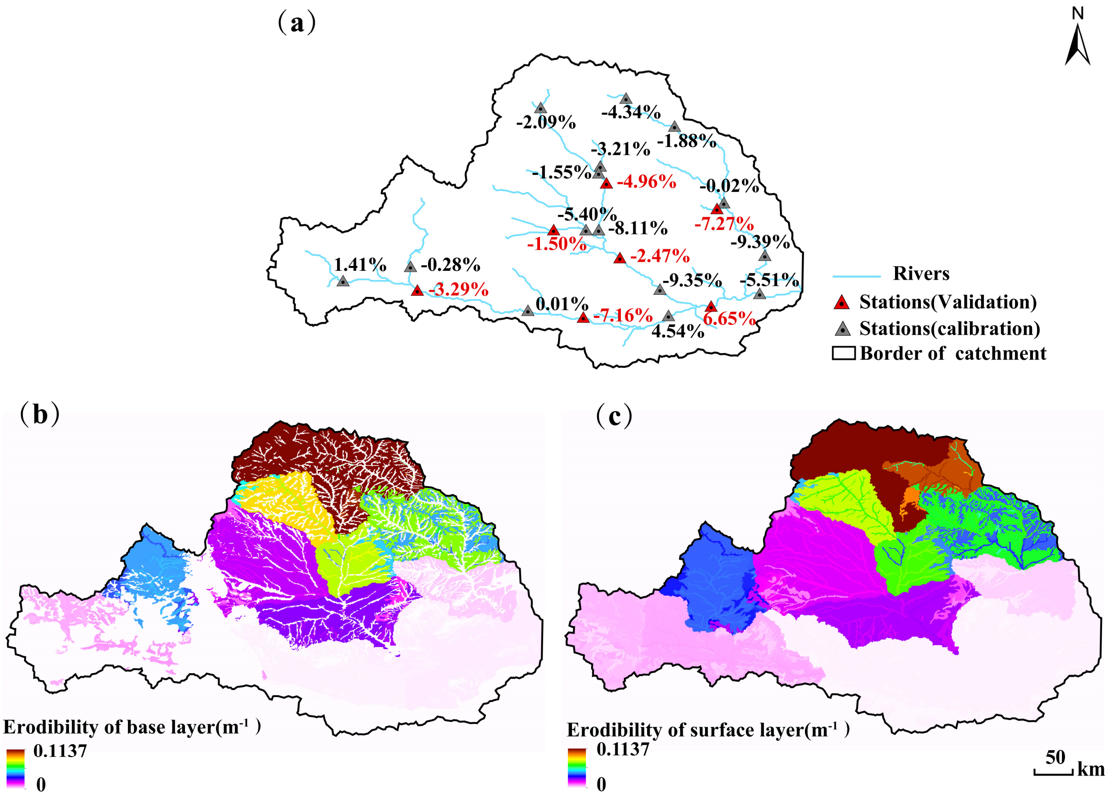

Fig S6 The difference between simulated and observed sediment load (a), and the distribution of erodibility of the base layer (b) and surface layer (c) after calibration

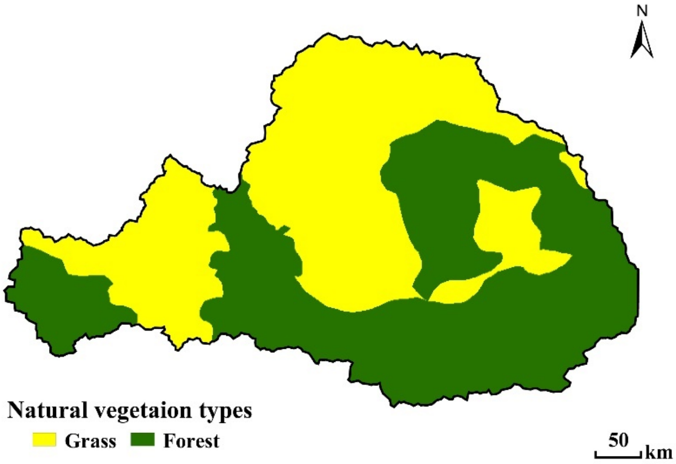

Fig S7 The distribution of natural vegetation types in Wei River catchment during the Holocene simulations

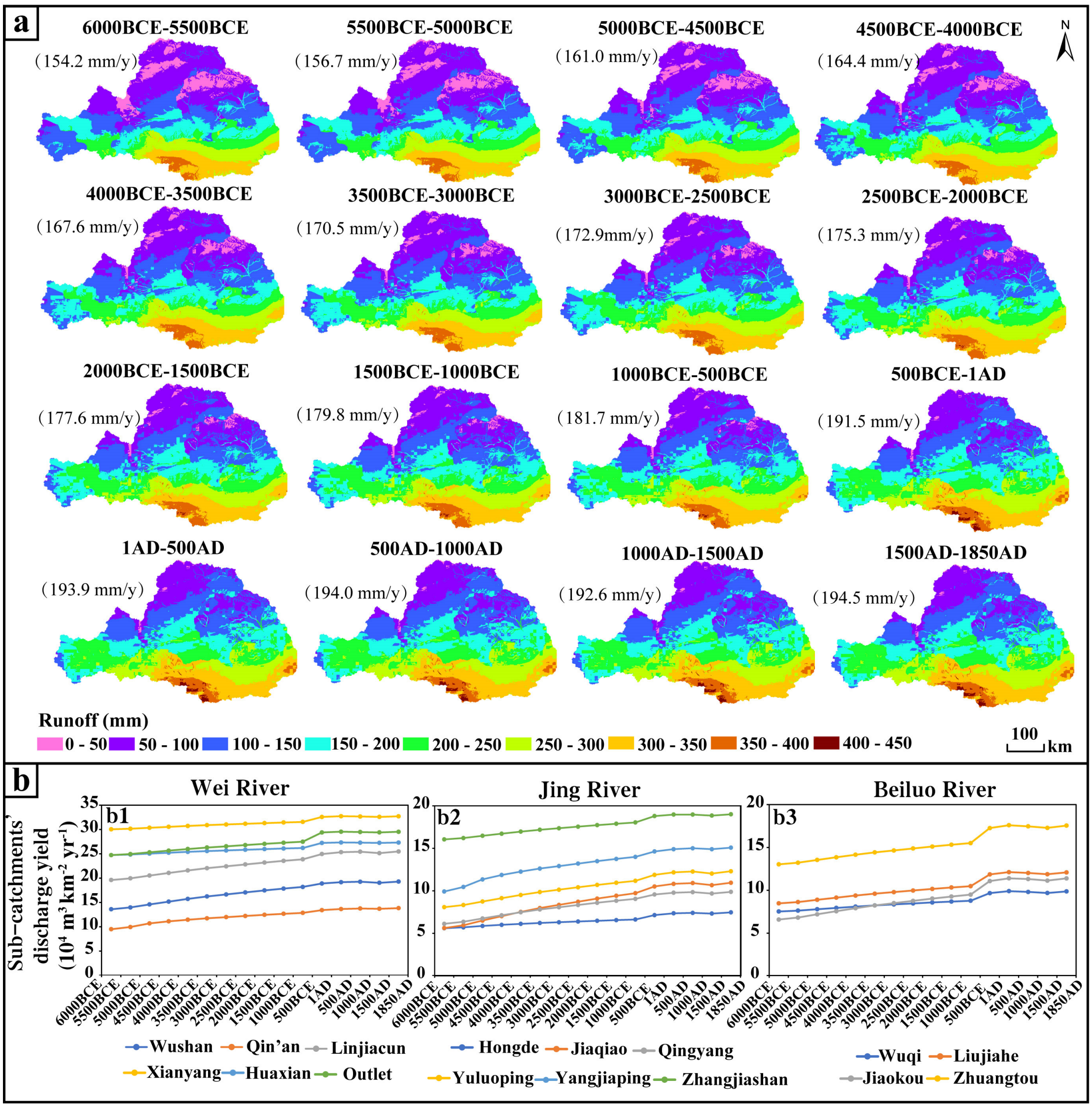

Fig S8 Simulated mean annual runoff (a) and the time trend of sub-catchment mean annual discharge (b) in the WCC Scenario.

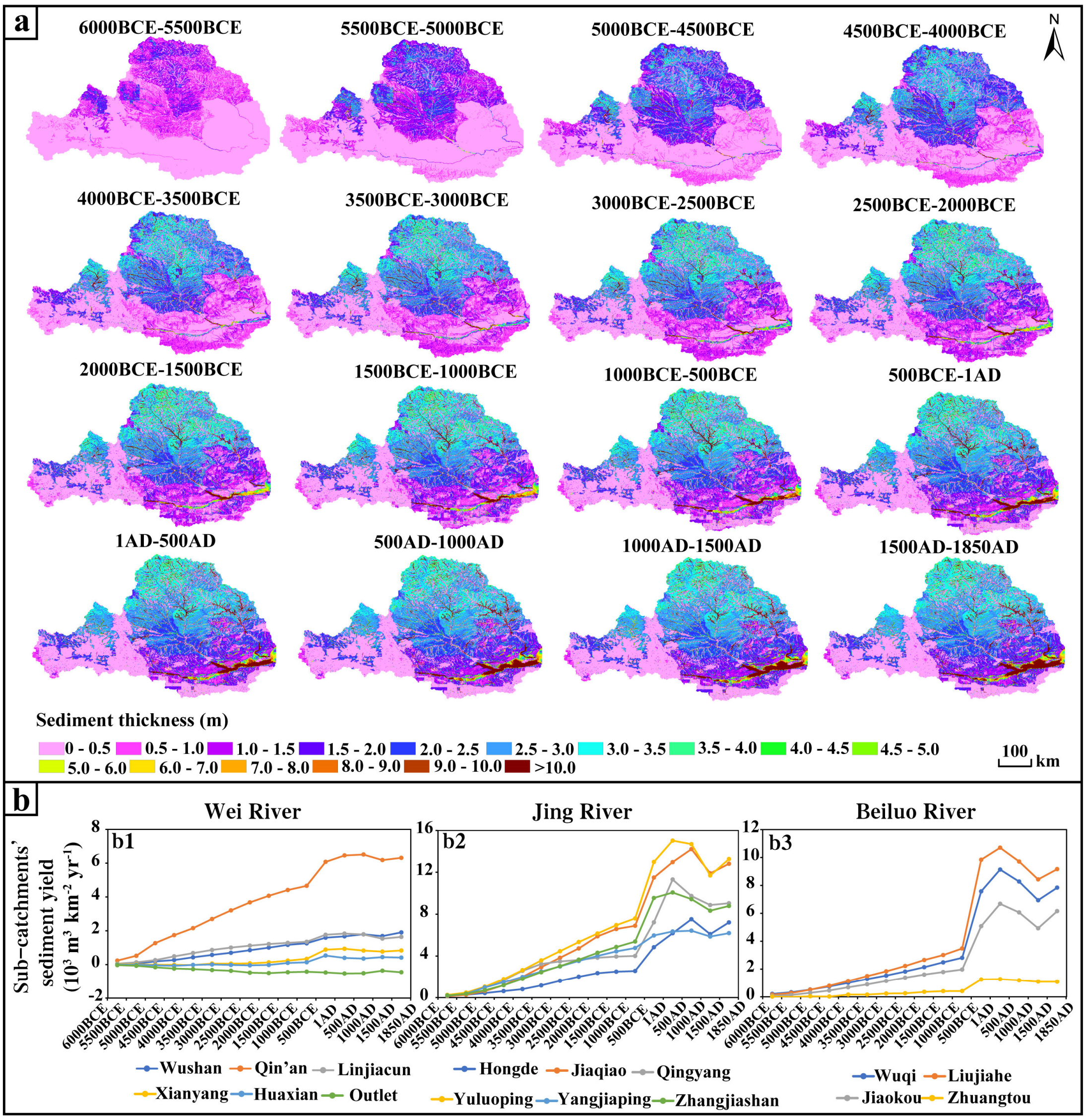

Fig S9 Sediment thickness (a) and the evolution of sub-catchment mean annual sediment yield (b) in the WCC Scenario

Table S1 Empirical model parameters used in evapotranspiration model

Parameters	Unit	Deciduous broadleaf forest	Grass	Crop
Annual leaf and fine root turnover fraction	**$1yr^{-1}$**	1.0	1.0	1.0
Annual live wood turnover fraction	**$1yr^{-1}$**	0.7	0.0	0.7
New leaf C : New fine root C	**kg C(kg C)$^{-1}$**	1.0	2.0	1.1
New stem C : New leaf C	**kg C(kg C)$^{-1}$**	2.2	0.0	1.7
New live wood C : New total wood C	**kg C(kg C)$^{-1}$**	0.1	0.0	1.0
New croot C : New stem C	**kg C(kg C)$^{-1}$**	0.2	0.0	0.0
Current growth proportion	**DIM**	0.5	0.5	0.5
C : N of leaves	**kg C(kg N)$^{-1}$**	24.0	24.0	24.0
C : N of fine roots	**kg C(kg N)$^{-1}$**	42.0	42.0	85.0
C : N of live wood	**kg C(kg N)$^{-1}$**	50.0	0.0	50.0
C : N of dead wood	**kg C(kg N)$^{-1}$**	442.0	0.0	200.0
Leaf litter labile proportion	**DIM**	0.39	0.39	0.39
Leaf litter cellulose proportion	**DIM**	0.44	0.44	0.44
Leaf litter lignin proportion	**DIM**	0.17	0.17	0.17
Fine root labile proportion	**DIM**	0.30	0.30	0.30
Fine root cellulose proportion	**DIM**	0.45	0.45	0.45
Fine root lignin proportion	**DIM**	0.25	0.25	0.25
Dead wood cellulose proportion	**DIM**	0.76	0.75	0.75
Dead wood lignin proportion	**DIM**	0.24	0.25	0.25
Canopy water interception coefficient	**1 LAI^{-1}day^{-1}**	0.041	0.021	0.0225
Canopy light extinction coefficient	**DIM**	0.70	0.60	0.60
All-sided to projected leaf area ratio	**LAI LAI^{-1}**	2.00	2.00	2.00
Canopy average specific leaf area	**$m^2kg^{-1}C^{-1}$**	30.00	45.00	35.00
Ratio of shaded SLA : sunlit SLA	**SLA SLA^{-1}**	2.00	2.00	2.00
Maximum stomatal conductance	**m s^{-1}**	0.005	0.01	0.005
Cuticular conductance	**m s^{-1}**	0.00001	0.00001	0.00001
Boundary layer conductance	**m s^{-1}**	0.01	0.04	0.03
Leaf water potential: start of conductance reduction	**Mpa**	-0.60	-0.60	-0.60
Leaf water potential: complete conductance reduction	**Mpa**	-2.30	-2.30	-2.30
Vapor pressure deficit: start of	**pa**	930.00	930.00	930.00
Vapor pressure deficit: complete	**pa**	4100.00	4100.00	4100.00

Table S2 Model parameters used in Landlab during the modern and Holocene simulations of the Wei River fluvial geomorphic evolution

Model parameters	Assigned values
Node spacing	1000 m
Time step	1 yr
Run time (modern simulation)	20 yr
Run time (Holocene simulation)	8000 yr
Initial H	0 m
Uplift rate (U)	0 m yr^{-1}
Diffusion coefficient (D)	0.05 m^2 yr^{-1}
Basement (bedrock) erodibility (K_r)	calculated using a geological map calibrated by natural sediment load (m^{-1})
Sediment erodibility (K_s)	calculated using a soil map calibrated by natural sediment load (m^{-1})
m	0.5
n	1
ω_{cr}	0 m yr^{-1}
ω_{cs}	0 m yr^{-1}
H_*	1 m
Porosity of bed sediment (ϕ)	0
Unitless fraction of fine sediment (F_f)	0
Net effective setting velocity (V)	2.0 m yr^{-1}

Table S3 Observed and reconstructed discharge and sediment data of each hydrological station in Wei River catchment

Rivers	Stations	Observed data (Zhang et al, 2007; Ran et al., 2012; Wang, 2013;Chen, 2017; Han, 2019)			The ratio of discharge	The ratio of sediment load	Reconstructed data (Chang et al., 2016)		
		Period	Discharge (m³)	Sediment load (t)			Period	Discharge (m³)	Sediment load (t)
Wei River	Wushan	1957-2000	5.56E+08	2.72E+07	25.20%	21.40%	1993-2010	6.51E+08	3.40E+07
	Qin'an	1957-2000	3.35E+08	5.04E+07	15.20%	39.70%	1993-2010	3.93E+08	6.31E+07
	Beidao	1957-2000	1.22E+09	1.18E+08	55.20%	92.90%	1993-2010	1.43E+09	1.48E+08
	Linjiacun*	1956-2000	2.21E+09	1.27E+08	100.00%	100.00%	1993-2010	2.58E+09	1.59E+08
	Weijiabao	1956-2000	2.94E+09	1.30E+08	69.70%	106.56%	1993-2010	3.85E+09	1.84E+08
	Xianyang*	1956-2000	4.22E+09	1.22E+08	100.00%	100.00%	1993-2010	5.52E+09	1.73E+08
	Lintong	1958-2000	6.83E+09	3.13E+08	96.70%	87.40%	1997-2010	8.57E+09	3.78E+08
	Huaxian*	1956-2000	7.06E+09	3.58E+08	100.00%	100.00%	1997-2010	8.86E+09	4.32E+08
Jing River	Hongde	1959-2016	6.40E+07	3.55E+07	4.10%	18.20%	1997-2010	6.51E+07	4.64E+07
	Jiaqiao	1959-2016	8.27E+07	1.76E+07	5.30%	9.00%	1997-2010	8.42E+07	2.30E+07
	Banqiao	1959-2016	1.40E+07	1.37E+06	0.90%	0.70%	1997-2010	1.43E+07	1.79E+06
	Qingyang	1959-2016	2.03E+08	7.18E+07	13.00%	36.80%	1997-2010	2.07E+08	9.38E+07
	Yuluoping	1959-2016	4.22E+08	1.06E+08	27.04%	54.30%	1997-2010	4.30E+08	1.38E+08
	Jingchuan	1959-2016	2.46E+08	1.27E+07	15.77%	6.50%	1997-2010	2.51E+08	1.66E+07
	Yangjiaping	1959-2016	6.58E+08	5.62E+07	42.16%	28.84%	1997-2010	6.70E+08	7.35E+07
	Jingcun	1959-2016	1.37E+09	1.82E+08	87.56%	93.32%	1997-2010	1.39E+09	2.38E+08
	Zhangjiashan*	1959-2016	1.56E+09	1.95E+08	100.00%	100.00%	1997-2010	1.59E+09	2.55E+08
Beiluo River	Wuqi	1963-2009	9.54E+07	2.82E+07	11.50%	40.29%	2002-2010	1.02E+08	4.03E+07
	Liujiahe	1959-2009	2.37E+08	5.88E+07	28.62%	84.00%	2002-2010	2.53E+08	8.40E+07
	Jiaokou	1967-2009	4.45E+08	6.58E+07	53.74%	94.00%	2002-2010	4.76E+08	9.40E+07
	Huangling	1967-2009	1.06E+08	3.31E+05	12.80%	0.47%	2002-2010	1.13E+08	4.73E+05
	Zhuangtou*	1957-2009	8.28E+08	7.00E+07	100.00%	100.00%	2002-2010	8.85E+08	1.00E+08

(The stations with * represent the compared objects included in the Chang et al. (2016))

Reference

Chang, J., Li, Y., Wei, J., Wang, Y. and Guo, A.: Dynamic changes of sediment load and water discharge in the Weihe River, China, Environ. Earth Sci., 75, 1-17, http://doi.org/10.1007/s12665-016-5841-9, 2016.

Chen, X.: Trend research of the lower reaches of the Wei River evolution in modern, MS thesis, Xi’an University of Technology, http://doi.org/CNKI:SUN:XBSZ.0.2019-01-012, 2017.

Han, X.: Spatial and temporal variation of runoff and sediment in Jing River basin and the influencing factors, MS thesis, Southwest University, https://kns.cnki.net/kcms2/article/abstract (last access: 8 January 2024), 2019.

Kaplan, J. O., Krumhardt, K. M., Ellis, E. C., Ruddiman, W. F., Lemmen, C. and Goldewijk, K. K.: Holocene carbon emissions as a result of anthropogenic land cover change, Holocene, 21, 775-791, https://doi.org/10.1177/0959683610386983, 2011.

Kuang, X., Han, Y. and Wang, Z.: Dynamic down scaling simulation of millennial climate in China since the last glacial maximum——climate comparison of three typical period, Quaternary Sci., 41, 842-855, http://doi.org/10.11928/j.issn.10017410.2021.03.18, 2021.

Ran, D., Zuo, Z., Wu, Y., Li, X. and Li, Z.: Streamflow and sediment load changes response to human activites in the middle reaches of the Yellow River, Science China Press, Beijing, China, ISBN: 9787030339331, 2012.

Wang, S.: Variation and regularity of water and sediment characteristics in the upper reaches of Wei River, Water Resour. Plan. Design, 9, 8-10, http://doi.org/10.3969/j.issn.1672-2469.2013.09.003, 2013.

Walling, D.: Human impact on land–ocean sediment transfer by the world's rivers, Geomorphology, 79, 192-216, http://doi.org/10.1016/j.geomorph.2006.06.019, 2006.

Zhang, C., Zhao, C., Yu, Z., Zhang, H., Zhou, A., Zhang, X., Feng, X., Sun, X. and Shen, L.: Western Pacific Ocean influences on monsoon precipitation in the southwestern Chinese Loess Plateau since the mid-Holocene, Clim. Dynam., 54, 3121-3134, http://doi.org/10.1007/s00382-020-05159-9, 2020.

Zhang, C., Zhao, C., Zhou, A., Zhang, H. and Chen, F.: Quantification of temperature and precipitation changes in northern China during the "5000-year" Chinese History, Quaternary Sci. Rev., 255, 106819, http://doi.org/10.1016/j.quascirev.2021.106819, 2021.

Zhang, H., Zhao, H., Gu, M. and Zhang, H.: Analysis of variation of water and sediment of Weihe basin in Shaanxi province, J. Yangling Vocat. Tech. College, 6, 1-4, http://doi.org/10.3969/j.issn.1671-9131.2007.02.001, 2007.